Development 133, 2167-2176 (2006) doi:10.1242/dev.02382

Multidirectional and multizonal tangential migration of GABAergic interneurons in the developing cerebral cortex

Daisuke H. Tanaka[1], Kazunori Maekawa[1], Yuchio Yanagawa[2], Kunihiko Obata[3] and Fujio Murakami[1,*]

Most GABAergic interneurons originate from the basal forebrain and migrate tangentially into the cortex. The migratory pathways and mode of interneuron migration within the developing cerebral cortex, however, previously was largely unknown. Time-lapse imaging and in vivo labelling with glutamate decarboxylase (GAD)67-green fluorescence protein (GFP) knock-in embryonic mice with expression of GFP in gamma-aminobutyric acid (GABA)ergic neurons indicated that multidirectional tangential (MDT) migration of interneurons takes place in both the marginal zone (MZ) and the ventricular zone (VZ) of the cortex. Quantitative analysis of migrating interneurons showed that rostrocaudally migrating neurons outnumber those migrating mediolaterally in both of these zones. In vivo labelling with a lipophilic dye showed that the MDT migration in the MZ occurs throughout the cortex over distances of up to 3 mm during a period of a few days. These results indicate that MZ cortical interneurons undergo a second phase of tangential migration in all directions and over long distances, after reaching the cortex by dorsomedial tangential migration. The MDT migration in the MZ may disperse and intermix interneurons within the cortex, resulting in a balanced distribution of interneuron subtypes.

KEY WORDS: Neuronal migration, Cortical interneuron, Time-lapse imaging, DiD labelling, Multidirectional tangential migration

INTRODUCTION

The orderly arrangement of neurons is crucial for normal CNS functioning. The CNS consists of compartments, such as the forebrain and the hindbrain, each of which possesses unique functions. Each compartment is composed of functional units, such as layers and nuclei. The function of these structures depends on the precise arrangement of neurons, including their synaptic connectivity. To establish highly ordered neuronal arrangements, neurons migrate from their site of origin to their final positions during development.

The cerebral cortex is responsible for higher brain functions. Its structure results from the orderly migration of two major types of neuron, the glutamatergic projection neurons and the GABAergic interneurons. Glutamatergic projection neurons arise in the germinal zones lining the lateral ventricle and migrate radially within the cortex toward the pial surface (for reviews, see Nadarajah and Parnavelas, 2002; Kriegstein and Noctor, 2004). The migration of GABAergic interneurons involves a more complex process, because most cortical interneurons originate from the ganglionic eminences (GEs) located in the subpallial telencephalon. These neurons first migrate tangentially toward the pallium and then populate the cortex (for reviews, see Marín and Rubenstein, 2001; Marín and Rubenstein, 2003; Parnavelas, 2000).

Although the migration from the GEs to the cortex is well documented, relatively little is known about the migration of interneurons within the cortex. During early development (from about E13.5 in mice), many interneurons in the lower intermediate zone/subventricular zone (IZ/SVZ) migrate dorsomedially towards the hippocampus (Anderson et al., 2001; Jimenez et al., 2002; Tanaka et al., 2003). Some of these cells appear to change their migratory direction, moving obliquely or radially toward the MZ (Tanaka et al., 2003). With the development of the cortical plate (CP; after about E15.5), various modes of radial migration can be seen: from the IZ and CP toward the pial surface (Tanaka et al., 2003); from the IZ-ventricular zone (VZ) to the ventricular surface (Nadarajah et al., 2002); and from the MZ toward the ventricle (Ang, Jr et al., 2003; Tanaka et al., 2003). These migration modes may be crucial in determining the final locations of the cortical interneurons. Most of these previous observations, however, were made in the coronal plane and therefore provide only fragmentary information about intracortical neuronal migration, particularly with respect to the tangential plane.

To clarify how cortical interneurons achieve appropriate locations within the mature cortex, a three-dimensional examination of interneuronal migrations is required. We, and others, recently carried out time-lapse imaging of MZ interneurons using a flat-mount cortical preparation and unexpectedly found that MZ interneurons migrate in all directions within the tangential plane (Ang, Jr et al., 2003; Tanaka et al., 2003). This finding tempted us to examine this migratory behaviour in a more systematic manner and quantitatively. Here, we show that multidirectional tangential (MDT) migration of interneurons takes place in multiple zones of the cortex, including the VZ. We further show that MDT migration occurs over long distances.

MATERIALS AND METHODS

Animals

We used heterozygous GAD67-GFP (Δneo) mice (Tamamaki et al., 2003; Tsunekawa et al., 2005), which will be referred to as GAD67-GFP mice. Experimental animals were obtained by mating female ICR mice with heterozygous male mice. GAD67-GFP embryos could be recognized by their GFP fluorescence. Noon of the day of vaginal plug detection was termed embryonic day (E) 0.5, and E19.5 was referred to as postnatal day (P) 0.

[1]Graduate School of Frontier Biosciences, Osaka University, and SORST, Japan Science and Technology Corporation (JST), Yamadaoka 1-3, Suita, Osaka 560-8531, Japan. [2]Department of Genetic and Behavioral Neuroscience, Gunma University Graduate School of Medicine, 3-39-22 Showa-machi, Maebashi 371-8511, Japan. [3]Neural Circuit Mechanism Group, BSI, RIKEN, Hirosawa 2-1, Wako, 351-0198, Japan.

*Author for correspondence (e-mail: murakami@fbs.osaka-u.ac.jp)

Accepted 29 March 2006

Although GAD65 (GAD2 – Mouse Genome Informatics), another isoform of GAD, is expressed at early corticogenesis (Lopez-Bendito et al., 2004) and could also contribute to GABA synthesis, we confirmed that more than 96% of GABA-immunoreactive neurons expressed GFP signal (n=458/471 and 1219/1270 at E13.5 and E15.5, respectively). Thus, GFP signal is expressed by almost all interneurons at these developmental stages. For some experiments, wild-type littermates or ICR mice (Clea Japan or SLC) were also used. All experiments were performed in accordance with the Osaka University Guidelines for the Welfare and Use of Laboratory Animals.

Real-time imaging in flat-mount preparations

Short-term (~2 hours) imaging

Real-time imaging of migrating GAD67-GFP-positive neurons (termed GFP neurons hereafter) in flat-mount preparations was performed as described previously (Tanaka et al., 2003). Briefly, neocortical tissues from E13.5 or E15.5 GAD67-GFP embryos were dissected and flat-mounted on membrane inserts with the ventricular side down or up to analyse the GFP neurons in the MZ or VZ, respectively, using a confocal microscope (MRC-1024; Bio-Rad). Images were taken from the tissue surface (at a depth of 0-50 μm for the MZ and 0-100 μm for the VZ) at 5 minutes intervals for 2-3 hours. A stack of images was created from a series of four to ten consecutive images taken along the z-axis at 10 μm intervals at every time point.

Long-term (>7 hours) imaging

Flat-mount preparations from neocortical wall were prepared as described above. They were transferred to the temperature- and gas-controlled incubation chamber (5% CO_2, 95% O_2 at 37°C) fitted onto a microscope stage (BX50, Olympus). The chamber was filled with Opti-MEM I reduced-serum medium containing 2.5% heat-inactivated fetal bovine serum, 2.5% heat-inactivated horse serum, 1% N2 supplement (all from Invitrogen), 20 mM D-glucose and 20 μg/ml streptomycin (Sigma). Labelled cells were viewed through a water-immersion objective (20, NA=0.5 each). Images were collected with a confocal microscope using 568 nm excitation and long-pass 585 nm emission filters. Images were taken from the tissue surface (at the depth of 0-100 μm) at 20-minute intervals. A stack of images was created from a series of 10 or 11 consecutive images taken along the z-axis at 12 or 14 μm intervals at every time point. Brightness and contrast were adjusted for every frame using Adobe Photoshop 7.0 software.

Quantitative analysis of migratory behaviour in real-time imaging

Data of real-time imaging that showed notable tissue movement was discarded. Because of the high density of GFP neurons, the analysis was carried out for all individually distinguishable GFP neurons. To analyse the rate and the direction of migration, a line was drawn connecting the position of a cell at the outset with its position at the end of observations, and the length and the angle of the line (medial direction was defined as 0° and rostral as 90°) were measured. Because almost all neurons migrated in a straight line during the observation period, the rate of migration was calculated by dividing the length of the line by the observation period (2-3 hours). For the analysis of directionality, the horizontal plane was subdivided into 24 or four sectors, and the proportion of migrating neurons in each sector was scored. The angle and mean rate of migration were measured for neurons with a rate of >5 μm/hour. Statistical analysis was done using the Mann-Whitney U-test or χ^2 test.

Observation of GFP neurons in tangential slices

Fixed GAD67-GFP brains (Tanaka et al., 2003) were embedded in 4% low-melting point agarose (Nacalai Tesque), and 50 μm-thick tangential slices were cut on a vibrating-blade microtome (VT-1000; Leica Microsystems), at around the level of the MGE along the rostrocaudal axis (Jimenez et al., 2002), and then mounted onto slides. Images were captured using a CCD camera (AxioCam; Zeiss) attached to an epifluorescence microscope (BX-60; Olympus) or by a confocal microscope (MRC-1024 or TCS SP2 AOBS; Leica Microsystems). The cortical zones were determined based on the density of GFP neurons.

In vivo analysis of DiD-labelled neurons

Pregnant mice were deeply anaesthetized with sodium pentobarbitone (Nembutal; Abbott; 100 mg/kg body weight) and laparotomies were performed to expose their uteri. After removing the uterine wall and opening the yolk sac of an embryo, a glass micropipette filled with 1,1′-dioctadecyl-3,3,3′,3′-tetramethylindodicarbocyanine (DiD; Molecular Probes) solution (100 mg/ml in dimethylformamide) was fitted to an injector (IM-30; Narishige); the pipe held vertically to the head of an embryo (E15.5) and inserted into the frontal, parietal or the occipital cortex, using a micromanipulator (Mk1; Singer instruments) under a dissecting microscope. A small opening was made on the yolk sac around the injection point to drain the amniotic fluid, which allowed us to make accurate injections. The injection (<0.1 μl) was performed into the parietal cortex so as not to label the LGE. After the injection procedure, embryos were repositioned into the abdominal cavity; the abdominal wall and the skin were then sutured.

Thirty-six or 72 hours after the injection procedure, embryos were removed and decapitated. Brains were fixed in 4% PFA in PB (0.1 M, pH 7.4) overnight at 4°C, and then transferred to phosphate-buffered saline (PBS; 0.1 M, pH 7.4) containing 0.1% EDTA and stored at 4°C. For flat-mount preparations, neocortical tissue encompassing the medial edge to the corticostriatal boundary was dissected and flat-mounted onto slides with the ventricular side down and coverslipped. For slice preparations, brains were embedded in 4% agarose (Nacalai Tesque), then sliced coronally or sagittally at 50 μm on a vibrating-blade microtome and stored at 4°C in PBS with 0.1% EDTA. The slices were transferred to slides and coverslipped.

Images were then captured using a confocal microscope (MRC-1024 or TCS SP2 AOBS). The following filter sets were used with the indicated wavelengths (in nm) for the excitation laser line and emission filters: GFP (green), 488/(504.5-539.5) with MRC-1024 or 488/(500-530) with TCS SP2 AOBS; DiD (far red), 647/(664-696) with MRC-1024 or 633/(650-730) with TCS SP2 AOBS. For the analysis of double labelling with DiD and GFP in individual neurons, the confocal pinhole was set to reduce the depth of optical sectioning as much as possible, and the same pinhole setting was used across channels to ensure equal section thickness for the different channels. Projection images were constructed from z-stacks (sets of stacked optical sections) for the analysis of morphology. Images were analysed using appropriate software supplied by the microscope manufacturer. Brightness and contrast were adjusted for every frame using Adobe Photoshop 7.0 software.

To examine the possibility that some DiD-labelled neurons had been labelled retrogradely, we injected DiD into fixed brains. For this, E18.5 GAD67-GFP embryos were removed from deeply anaesthetized pregnant mice and decapitated. Brains were then removed and DiD was injected into the dorsal cortex as described above. The brains were fixed immediately in 4% PFA in PB with 0.1% EDTA and kept in the fixative in the dark at room temperature (RT) over one month. Slices were then prepared and imaged as described above.

Quantitative analysis of DiD-labelled GFP neurons

Because a high density of labelled neurons near the injection site interfered with the analysis, the analysis was carried out for all DiD-labelled GFP neurons located >400 μm or >600 μm from the injection site in slices or flat-mount preparations, respectively.

Slice preparations

The length of a straight line connecting the position of each DiD-labelled GFP neuron and the injection site (the point in the same zone) was defined as the migration distance. The distance thus measured should be an underestimate because the curved contour of the cortex. The zonal position of DiD-labelled GFP neurons was determined referring to the GAD67-GFP cell distribution pattern, which could be correlated to the pattern by Nissl staining (Tanaka et al., 2003).

Flat-mount preparations

The length and the angle of a straight line connecting the injection site and the position of each DiD-labelled GFP neuron were measured. The DiD-labelled GFP neurons located medial to the injection site could not be analysed because the injection had to be made into the dorsal cortex, and the region of the cortex medial to the injection site (including the cingulate cortex) could not be flattened because of folding of the cortex. For the same reason, a part of the rostral or caudal region could not be analysed when the injection was administered into the frontal or occipital cortex, respectively. The curved structure of the cortex also interfered with the analysis of neurons located far from the injection site.

Exo utero electroporation and immunostaining of Red fluorescent protein-labelled cells

We performed exo utero electroporation on E12.0 embryos. Red fluorescent protein (DsRed2; Clontech) expression vector with a CAG promoter (Hatanaka et al., 2004; Hatanaka and Murakami, 2002; Niwa et al., 1991) was dissolved in PBS at a concentration of 0.5 μg/μl. Immediately before use, Fast Blue solution (0.1% in PBS; Nacalai Tesque) was added to the plasmid solution at a ratio of 1:10 to monitor the injection. Plasmid solution (~1 μl) was injected into the lateral ventricle using a glass micropipette fitted to an injector (IM-30; Narishige). The embryo's head was clasped with forceps-shaped electrodes (CUY650P2; Unique Medical) connected to a square-pulse generator (CUY21; TOKIWA or ECM830; BTX) with an angle of 30-60° from the brain's horizontal plane for GE-directed electroporation. Electric pulses (30 V, 50 mseconds, 5 times, 950 mseconds intervals) were then delivered.

Three and half days after the electroporation, embryos were removed and decapitated. Brains were fixed in 4% PFA in PB overnight at 4°C, and subjected to cryosectioning. Cryosections (20-30 μm thickness) were mounted onto slides (12-550-15; Fisher Scientific) and incubated in 5% NGS and 0.3% Triton-X in PBS (NGS/TX/PBS) for 1 hour, followed by 4 hours incubation in a rabbit polyclonal anti-LHX6 antibody (1/500; generous gift from Dr V. Pachnis, University College, London) in NGS/TX/PBS at room temperature. Sections were then incubated with a goat FITC-conjugated anti-rabbit IgG antibody (1/25; Jackson ImmunoResearch) for 1 hour at room temperature in PBS and examined using confocal microscopy (TCS SP2 AOBS).

Co-culture of cortical slices

A cortical slice from a P0 wild-type mouse was co-cultured with that from a P0 GAD67-GFP animal. P0 brains from wild-type or GAD67-GFP heterozygous mice were dissected, embedded in 4% low-melting point agarose in PBS, and the dorsolateral part of the cortex sliced coronally on a vibrating-blade microtome at 250 or 300 μm in Hanks' solution. The MZ of a wild-type slice was placed adjacent to that of a GAD67-GFP slice and cultured on a membrane insert (Millicell-CM PICMORG50; Millipore) coated with rat tail collagen, in Opti-MEM I reduced-serum medium containing 2.5% heat-inactivated fetal bovine serum, 2.5% heat-inactivated horse serum, 1% N2 supplement (all from Invitrogen, Grand Island, NY), 20 mM D-glucose, and 20 μg/ml streptomycin (Sigma). After a culture period of one day, the slice was fixed with 4% PFA in PB overnight, immersed in 20% sucrose in PB for six hours to overnight (each at 4°C), put in glass tubes containing 20% sucrose in PB, frozen with liquid nitrogen and thawed. Following washes with PBS, double immunofluorescence labelling was performed. Slices were first incubated with a rat anti-GFP monoclonal antibody (1:1000; Nacalai Tesque) overnight, followed by incubation with a mouse anti-MAP2 monoclonal antibody (HM-2; 1:2000; Sigma) overnight. Then, the slices were reacted in goat biotinylated anti-mouse IgG (1/500; Jackson ImmunoResearch, West Grove, PA) for six hours, followed by six hours incubation in goat Alexa488-conjugated anti-rat IgG antibody (1/200; Jackson ImmunoResearch), then with Alexa594-conjugated streptavidin (1/200; Jackson ImmunoResearch). All antibodies were diluted in PBS containing 0.3-0.5% Triton X-100. Normal goat serum (5%) was added to the primary and secondary antibody solutions. All reactions were carried out at room temperature. Immunofluorescent localization was examined using a confocal microscope (TCS SP2 AOBS; Leica Microsystems).

RESULTS

MDT migration of interneurons in multiple cortical zones

In our previous time-lapse analysis of coronal slices, mediodorsal migration was only observed in the IZ/SVZ. However, MDT migration of interneurons was observed in the MZ in flat-mount preparations when viewed from the dorsal surface (Tanaka et al., 2003). This raises the possibility that migrations in directions other than mediodorsal might also occur in deeper cortical zones. To address this issue, we cut serial tangential sections from fixed cortices of E15.5 GAD67-GFP mice (Fig. 1A,B) and examined the orientation of the leading processes of GFP neurons. As expected, the leading processes of GFP neurons in the CP, subplate (SP) and VZ were oriented in many directions (Fig. 1C2-C5,C10,C11), with

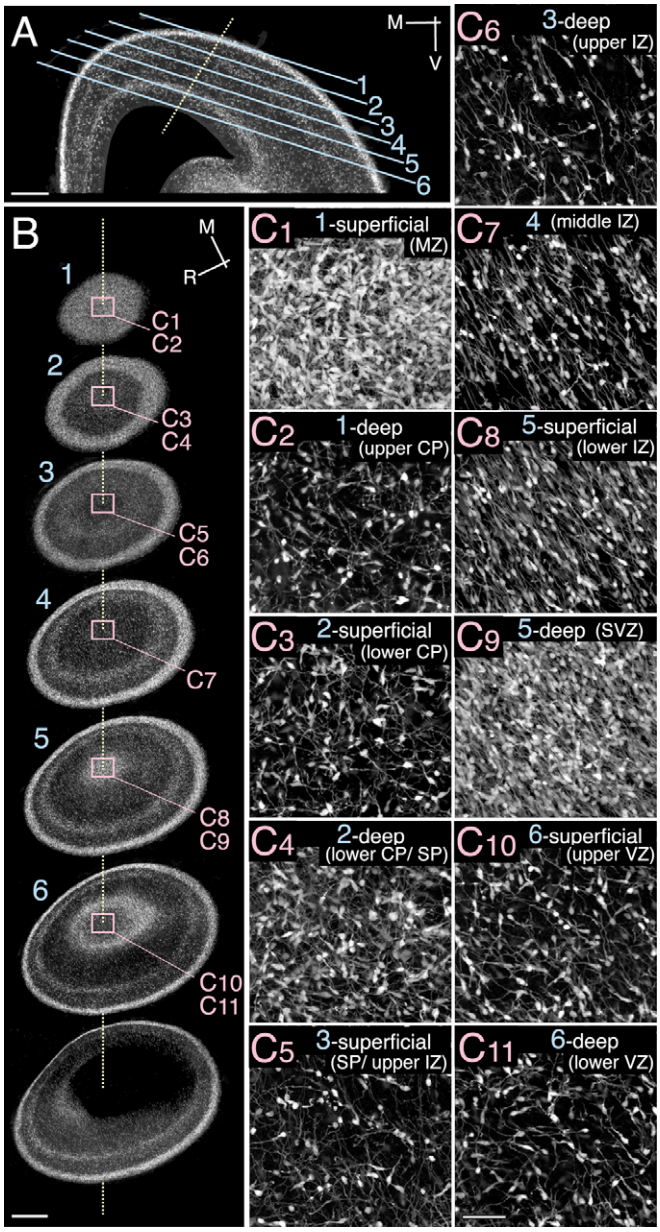

Fig. 1. Cortical interneurons orient in many directions in multiple zones. (**A**) Semi-schematic representation of a transverse section of an E15.5 GAD67-GFP mouse cortex indicating the depth of tangential sections. Numbered blue lines represent the approximate level of the cortex from which the corresponding tangential sections in B were obtained. Dotted line indicates the central region of the sections indicated by boxes in B. (**B**) GFP neurons in E15.5 serial tangential sections, lined from pial to ventricular side. (**C**) Higher magnification confocal images of the boxed areas in B. Two images were taken from each section by changing the depth of focus. C1, C3, C5, C8 and C10 were taken from the dorsal part of tangential slices numbered 1, 2, 3, 5 and 6 in B, respectively. C2, C4, C6, C9 and C11 were from the ventral part of slices numbered 1, 2, 3, 5 and 6 in B, respectively. GFP neurons orient in many directions in the MZ, CP, SP and VZ. M, medial; V, ventral; R, rostral. Scale bars: A, 200 μm; B, 400 μm; C, 40 μm.

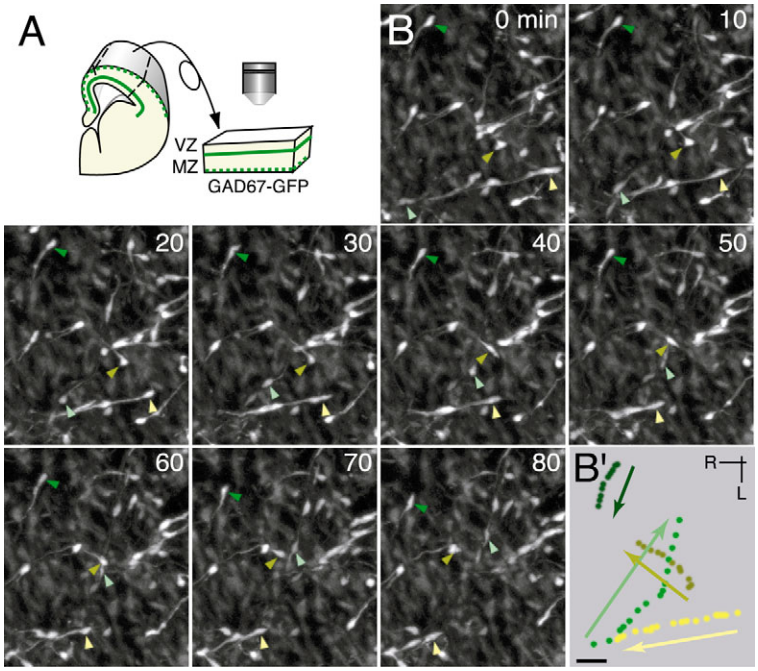

Fig. 2. Time-lapse analysis of MDT migration of interneurons in the VZ. (**A**) Schematic of time-lapse imaging in a flat-mount preparation. Dorsal cortex was excised and flat-mounted with the ventricular side up. (**B**) Confocal images of interneurons in the VZ of an E13.5 mouse viewed from the ventricular side. The number in the top right corner is the time in minutes. Neurons indicated by arrowheads of the same colour represent the same neurons. (B′) Tracks of the four neurons shown in B. Each dot corresponds to the neurons shown by arrowheads in B and illustrates their positions plotted at 5 minutes intervals. Arrows indicate the direction of migration. R, rostral; L, lateral. Scale bar: 20 μm.

most IZ processes oriented mediodorsally (Fig. 1C5-C8). Although recognition of the processes of individual neurons in the MZ and SVZ was blurred because of the high cell density, it appeared that MZ interneurons were oriented in all directions (Fig. 1C1), and SVZ neurons were only weakly oriented in the mediodorsal direction (Fig. 1C9). Similar results were obtained for E13.5, E14.5 and E16.5 animals, although the orientation of most CP neurons at E16.5 could not be clearly determined, perhaps because many were radially oriented (data not shown). These morphological features raise the possibility that MDT migration would also occur in deeper zones.

To directly test this idea, MDT migration in deeper zones was examined with time-lapse analyses of VZ neurons using flat-mount preparations viewed from the ventricular surface (Fig. 2A). As exemplified in Fig. 2B, VZ neurons migrated vigorously in all directions. VZ MDT migration was observed at both E13.5 (n=11; Fig. 2B,B′; see also Movies 1 and 2 in the supplementary material) and E15.5 (n=8; see Movie 3 in the supplementary material), consistent with the observations in fixed preparations. Collectively, these observations suggest that MDT interneuron migration occurs widely across zones of the developing cortex.

A majority of interneurons in the MZ and VZ migrate rostrally or caudally

MZ interneurons show robust MDT migration in flat-mount cortical preparations (Tanaka et al., 2003). This observation is inconsistent with the view that the MZ is a major pathway for mediodorsal migration (de Carlos et al., 1996; Jimenez et al., 2002; Lavdas et al., 1999; Polleux et al., 2002). One possible explanation is that a significant number of MZ interneurons migrate in directions other than mediodorsal, although most do migrate mediodorsally. To examine this possibility, we performed a quantitative analysis of the direction of the GFP migration on previously recorded images taken from the dorsal cortex of E13.5 mice (Tanaka et al., 2003). We first scored the migrating neurons by subdividing the horizontal plane into 24 sectors, and we counted the proportion of the migrating neurons in each sector (n=1132 neurons, five hemispheres). The tendency for the population was rostrocaudal migration (Fig. 3A). Comparisons of the migrations in the four quadrants (medial, rostral, lateral and caudal directions) indicated that the proportion of rostrally migrating neurons was significantly greater than that of medially migrating neurons (U-test; P<0.01; Fig. 3B, left panel); The proportion of either rostrally or caudally migrating neurons was significantly greater than that of either medially or laterally migrating neurons (U-test; P<0.01; Fig. 3B, right panel). To examine whether migration in the VZ is also biased in specific direction(s), a similar quantitative analysis for GFP neurons was carried out in the VZ (n=474 neurons, four hemispheres). Although the interneurons also migrated in all directions (Fig. 3C), the proportion of laterally migrating neurons was less than that in other directions (Fig. 3D, left panel). VZ interneurons also appeared to prefer rostrocaudal directions rather than mediolateral directions (U-test; P<0.03; Fig. 3D, right panel), although VZ interneurons tended to migrate medially rather than laterally. These results suggest that a majority of MZ and VZ interneurons migrate rostrocaudally.

Cortical interneurons migrated faster (U-test; P<0.02) in the VZ (23.7±0.5 μm/hour; four hemispheres) than in the MZ (18.8±0.9 μm/hour; five hemispheres), suggesting that interneurons have different motilities in different zones. Average migration rates did not differ for neurons migrating in different directions within each zone (MZ: χ^2=3.01, P>9.99; VZ: χ^2=12.59, P>0.9).

Long-distance migration of interneurons within the cortex

The physiological significance of cortical MDT migration is unclear. One possibility is that it contributes to interneuron dispersion within the cortex. MDT migration of interneurons should then occur over long distances, a possibility that cannot be examined with time-lapse analysis in short time windows. We therefore performed in vivo DiD injections into the parietal cortices of E15.5 GAD67-GFP mice (Fig. 4A,B), and analysed the distribution of DiD-labelled GFP neurons after survival of a few days. One and a half days after injection, some DiD-labelled GFP neurons were found in sagittal sections far from the injection site (>400 μm; Fig. 4B′). DiD-labelled GFP neurons were also observed medially and laterally, far from the injection sites in

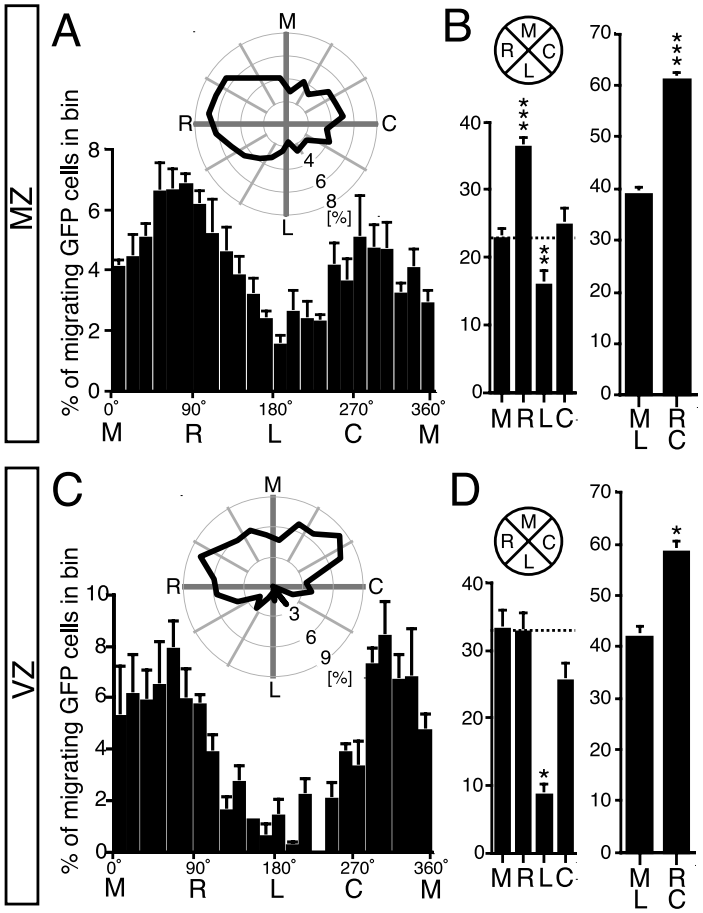

Fig. 3. Quantitative analysis of MDT migration of interneurons in the MZ and VZ. (**A**,**B**) Quantification of the migration direction of GFP neurons in the MZ. Most GFP neurons migrated (80±1%; *n*=1132/1412 neurons, five hemispheres; see Materials and methods for the definition of migrating neurons). 0° represents medial and 90° rostral migration. The horizontal plane was subdivided into 24 (A), four (B, left panel) or two sectors (B, right panel), and the proportion of the neurons migrating in each sector was analysed (*n*=1132 neurons, five hemispheres). The proportion of neurons in each sector is shown by the histogram (average±s.e.m.). Note that rostrally migrating neurons outnumber those migrating medially (B, left panel). (**C**,**D**) As for A and B, but for VZ GFP neurons. Almost all GFP neurons migrated (96±2%; *n*=474/496 neurons, four hemispheres). In the upper part of A and C, overall distribution is also shown by polar coordinates. All data were from E13.5 mice. **P*<0.03, ***P*<0.02, ****P*<0.01 (Mann–Whitney U-test). M, medial; R, rostral; L, lateral; C, caudal.

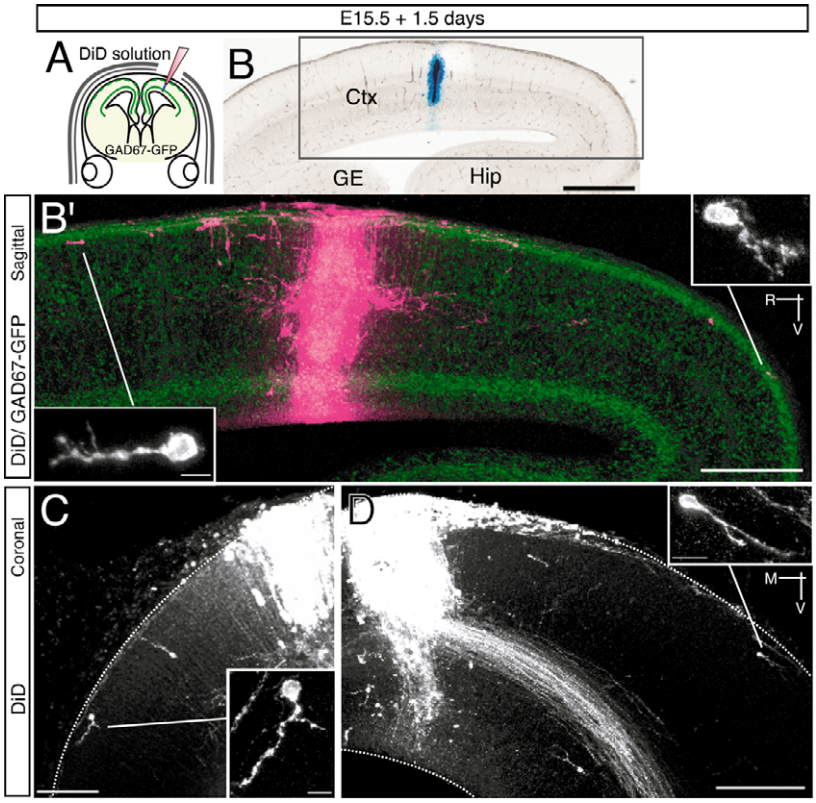

Fig. 4. DiD-labelled GFP neurons with migrating cell morphology rostral, caudal, medial and lateral to injection site. (**A**) Schematic of an embryonic mouse brain illustrating DiD injection into the parietal cortex. Injection was performed at E15.5. (**B**) Transmitted-light image of a sagittal slice from a DiD-injected GAD67-GFP brain one and a half days after injection. (B9) Fluorescent micrograph showing the distribution of DiD-labelled GFP neurons in the boxed area in B. DiD labelling (magenta) was confined to the cerebral cortical wall. Merged view of GFP and DiD fluorescence. Insets show higher magnification views of the DiD-labelled GFP neurons indicated by straight lines. (**C,D**) Fluorescent micrographs showing DiD-labelled neurons in coronal sections one and a half days after injection. Insets show higher magnification views of the DiD-labelled GFP neurons indicated by straight lines. Both show the morphology of migrating neurons extending leading processes. Ctx, cortex; GE, ganglionic eminence; Hip, hippocampus; R, rostral; M, medial; V, ventral. Dotted lines indicate the slice outline. Scale bars: B, 500 μm; B′, 300 μm; C, 100 μm; D, 200 μm; B9,C,D, insets, 10 μm.

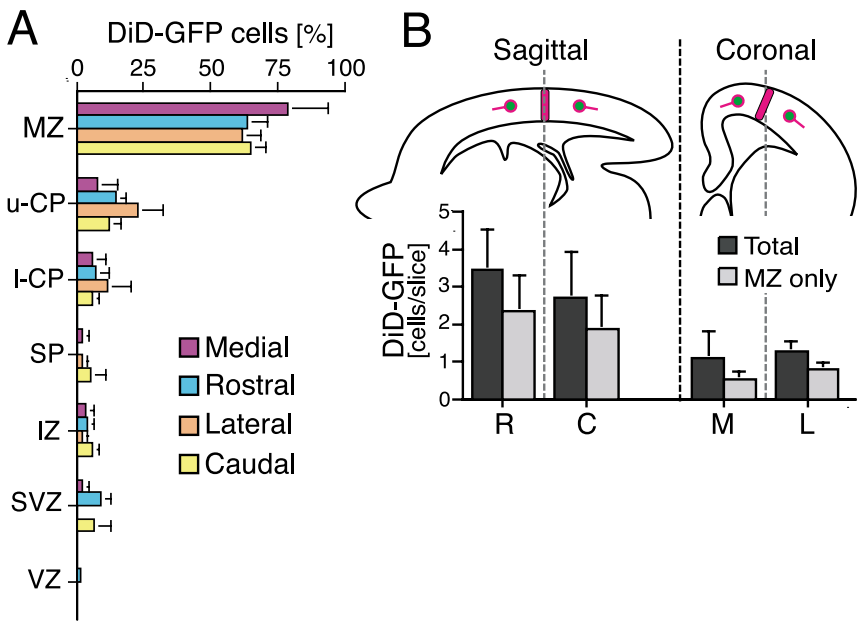

Fig. 5. Distribution of DiD-labelled GFP neurons in sagittal and coronal slices, one and a half days after injection. The analysis was carried out for all DiD-labelled GFP neurons located >400 μm from the injection site in sagittal (*n*=166 neurons, four brains) or coronal sections (*n*=74 neurons, four brains). (**A**) Percentage of DiD-labelled GFP neurons distributed in each cortical zone. The neurons were subdivided into four classes based on their position relative to the injection site: medial (purple), rostral (light blue), lateral (orange) or caudal (yellow). MZ, marginal zone; u-CP, upper cortical plate; l-CP, lower cortical plate; SP, subplate; IZ, intermediate zone; SVZ, subventricular zone; VZ, ventricular zone. (**B**) DiD-labelled GFP neurons observed rostral and caudal to the injection site in sagittal sections (left), or medial and lateral to the injection site in coronal sections (right). M, medial; R, rostral; L, lateral; C, caudal.

coronal sections (Fig. 4C,D). Some of these DiD-labelled GFP neurons had a leading process oriented away from the injection site (insets of Fig. 4B′,C,D). These results suggest that tangential migration of interneurons occurs over long distances within the cortex.

The long-distance tangential migration of interneurons revealed by the DiD injection appeared concentrated in the MZ and occurred in rostrocaudal directions rather than mediolateral directions. About 60% of the DiD-labelled GFP neurons in sagittal sections (Fig. 5A, blue and yellow bars), and about 70% of the DiD-labelled GFP neurons in coronal sections (Fig. 5A, purple and orange bars) were found in the MZ. The labelled neurons did not appear to have either rostral or caudal directional biases (Fig. 5B, left dark bars). Likewise, they did not appear to have either medial or lateral directional biases (Fig. 5B, right dark bars). The number of DiD-labelled GFP neurons (per section) in parasagittal sections was larger than for coronal sections (Fig. 5B, dark bars). The results were similar when the labeled neurons in the MZ were analysed (Fig. 5B, light bars).

To obtain an overview of tangential migration in the MZ, cortical flat mounts were prepared from DiD-injected GAD67-GFP brains (Fig. 6A). One and a half days after injection (E17.0), a substantial number of DiD-labelled GFP neurons (*n*=38 neurons, two brains) were seen in many directions, some more than 600 μm from the injection sites (Fig. 6B1,D). Most DiD-labelled GFP neurons had a trailing process and a leading process with a few branches (Fig. 6B2,B3), a morphology typical for migrating MZ interneurons (Tanaka et al., 2003) (Fig. 9B, see also Movie 4 in the supplementary material). Three days after the injection procedure (E18.5), many DiD-labelled GFP neurons (*n*=119 neurons, six brains) were found even further from the injection site (>800 μm; Fig. 6C,D); some of these neurons were more than 1.5 mm from the injection site (Fig. 6C1,D). DiD-labelled GFP neurons had many orientations (Fig. 6B,C). Many neurons were distributed in rostral, caudal and lateral directions, although we could not compare the distribution of DiD-labelled GFP neurons in all directions because of folding of the cortex (see Materials and methods).

Similar dispersions of DiD-labelled GFP neurons were observed after DiD injections into the frontal (Fig. 7A) or the occipital cortices (Fig. 7B) (*n*=2 each). Many DiD-labelled GFP neurons were located caudolateral to frontal injection sites (Fig. 7A,C) but rostrolateral to the occipital injection sites (Fig. 7B,D). In both cases, a substantial number of neurons were found more than 2 mm from the injection site (Fig. 7C,D). Together, these results suggest that the MDT migration of interneurons takes place over long distances and across cortical areas.

Cortical interneurons appear to migrate toward the ventricle and enter the CP after dispersing throughout the MZ. Twelve per cent of DiD-labelled GFP neurons in parasagittal sections from DiD-injected brains had leading processes directed towards the ventricle (*n*=18/151 DiD-labelled GFP neurons, three brains; see Fig. S1A,B in the supplementary material). Similar results were obtained in coronal sections (*n*=6/145 DiD-labelled GFP neurons, two brains; see Fig. S1C in the supplementary material). All of these neurons were found in the MZ or upper CP, at various distances from the injection site (see Fig. S1D in the supplementary material). Ventricle-directed migration of MZ interneurons was also observed in co-culture experiments with postnatal neurons (see Fig. S2 in the supplementary material).

MGE-derived interneurons migrate in many directions within the MZ

Cortical interneurons have multiple origins (Anderson et al., 2001; Anderson et al., 1997; Butt et al., 2005; Lavdas et al., 1999; Nery et al., 2002; Wichterle et al., 2001; Xu et al., 2004), raising the possibility that directionality of MZ interneurons is correlated with their origin. To test this, we introduced *DsRed*-coding plasmid into the E12.0 MGE using the electroporation-based in vivo gene transfer technique (Fig. 8A, inset). At E15.5, 3.5 days after the electroporation, DsRed-labelled cells have arrived at the neocortex (Fig. 8A). Most of them were positive for both GAD67-GFP (98.1±1%; Fig. 8B) and LHX6 (91.4±7%, Fig. 8C), indicating that these interneurons were derived from the MGE (Anderson et al., 2001; Lavdas et al., 1999; Sussel et al., 1999).

Real-time imaging of E15.5 MZ (Fig. 9A) shows DsRed cells migrating in all directions (Fig. 9B-B″, see also Movie 4 in the supplementary material), with no obvious directional bias. This observation demonstrates that GABAergic interneurons from at least one specific site, the MGE, can migrate in many directions within the MZ.

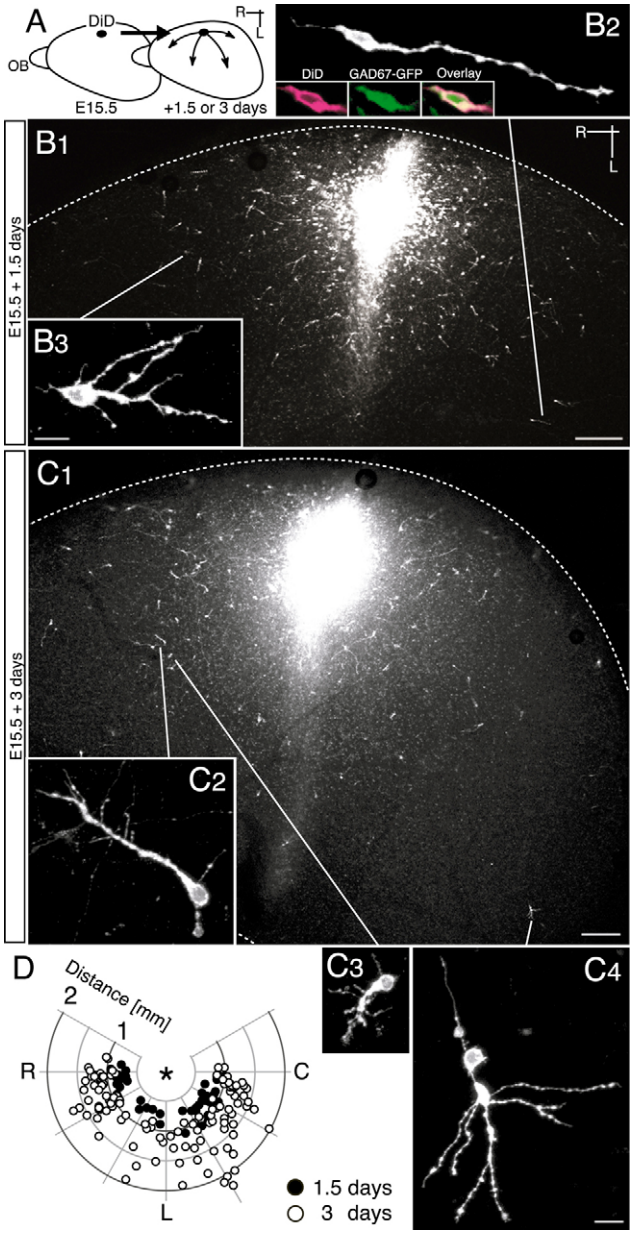

Fig. 6. Dispersion of DiD-labelled GFP neurons in the MZ after DiD injection into the parietal cortex. (**A**) Schematic of the experimental paradigm used. DiD-labelled GFP neurons in the MZ were analysed after an appropriate survival period by preparing flat-mount cortical preparations. About 70% of DiD-labelled neurons expressed GFP (*n*=352/485 DiD-labelled cells, 12 brains). The remainder may include Cajal-Retzius cells (Bielle et al., 2005; Takiguchi-Hayashi et al., 2004). (**B**,**C**) Distribution of DiD-labelled neurons in flat-mount preparations one and a half days (E17.0; B) or three days (E18.5; C) after injection. (B1) Dorsal view of the area around the injection site. (B2,B3) Higher magnification of the DiD-labelled GFP neurons indicated by straight lines in B1. These neurons extended an unbranched (B2) or branched (B3) leading process and a short trailing process. Comparison of fluorescence in a single optical section demonstrates that this DiD-labelled cell (inset, magenta) expresses GFP (green). (C1) Dorsal view of the area around the injection site. (C2-C4) Higher magnification of the DiD-labelled GFP neurons indicated by straight lines in C1. These neurons showed typical morphology of migrating neurons in the MZ extending a leading process (C2), occasionally extending a thick but short process (C3) that appears to elongate toward the CP (data not shown). Neurons having several long processes, and granular structure in the trailing process were also observed (C4). (**D**) Distribution of DiD-labelled GFP neurons in flat-mount preparations one and a half (E17.0; black circles) and three days (E18.5; white circles) after injection. The neurons situated >600 μm or >800 μm from the injection site were plotted for E17.0 or E18.5 brains, respectively. Pooled data from two (E17.0) or six (E18.5) independent experiments. The lack of data medial to the injection site is due to folding of the cortex. OB, olfactory bulb; R, rostral; C, caudal; L, lateral. Dotted lines, flat-mount outline. Scale bars: in B1,C1, 200 μm; in B2, B3, 10 μm; in C2-C4, 10 μm.

DISCUSSION

The present study demonstrated that MDT migration of cortical interneurons occurs across multiple zones of the developing cortex. In the MZ, as well as in the VZ, these neurons primarily migrated rostrocaudally. We also found that interneurons in the MZ migrate over long distances (1-3 mm), not merely drifting locally.

Technical considerations

As DiD can be transported retrogradely, it is possible that GFP neurons observed here were labelled retrogradely from the injection site. However, we do not think it likely because: (1) most DiD-labelled GFP neurons extended short trailing processes that did not reach the injection site (Figs 4, 6, 7); (2) DiD injection into the cortex of E18.5 GAD67-GFP mice followed by immediate fixation caused many retrogradely labelled GFP neurons, but most of them were confined to the vicinity of the injection site (<400 μm) (K.M., D.H.T. and F.M., unpublished); (3) many DiD-labelled GFP neurons had morphological features characteristic of migrating cortical neurons, extending a branched or unbranched leading process and a trailing process (Nadarajah et al., 2002; Nadarajah et al., 2003; Nadarajah et al., 2001; Noctor et al., 2004; Polleux et al., 2002; Tabata and Nakajima, 2003; Tanaka et al., 2003); (4) the distance of DiD-labelled GFP neurons from the injection site observed after three days survival (viz, 1-3 mm; Fig. 6C,D, Fig. 7) translates into a rate of 14-42 μm/hour, which is comparable to the average rate of GFP cell migration, observed in the present time-lapse imaging in the MZ, of 19 μm/hour.

MDT migration of cortical interneurons in multiple zones

Our observation in fixed preparations suggested the occurrence of multizonal MDT migration. This was directly demonstrated by performing real-time analysis of VZ interneurons, which migrated in many directions (Fig. 2, Fig. 3C,D). Our findings agree with a previous study in cortical explants that showed DiI-labelled cells near the ventricular surface migrating in all directions (Fishell et al., 1993). Although most of the labelled cells in that study appeared to be progenitor cells, it is possible that some were interneurons.

Because of technical limitations, it was not possible to carry out real-time analysis for interneurons in zones other than the MZ and VZ. However, the orientation of interneurons in fixed preparations is consistent with the notion that MDT migration also occurs in the CP and SP (Fig. 1).

MDT migration of cortical interneurons over long distances

Our DiD-injection experiments demonstrate that cortical interneurons can migrate long distances (1-3 mm) in the MZ (Figs 6, 7). Thus, it is likely that the MZ GFP neurons observed with

real-time imaging (Tanaka et al., 2003) (Fig. 3A,B) are undergoing long-distance migrations rather than local movements.

VZ interneurons also appear to migrate long distances. DiD injections into the cortex labelled only a small number of VZ neurons more than 400 μm from the injection sites (Fig. 5A). However, because we attempted to avoid DiD injections into the ventricle, the centres of the injections tended to be located in the superficial parts of the cortical wall. The poor DiD labelling in the VZ is perhaps therefore due to injection sites that were not close enough to the VZ. Indeed, when DiI was focally injected into the VZ and SVZ of the developing ferret cortex, neurons in these zones, possibly including interneurons, tangentially migrated more than 2.5 mm (O'Rourke et al., 1997).

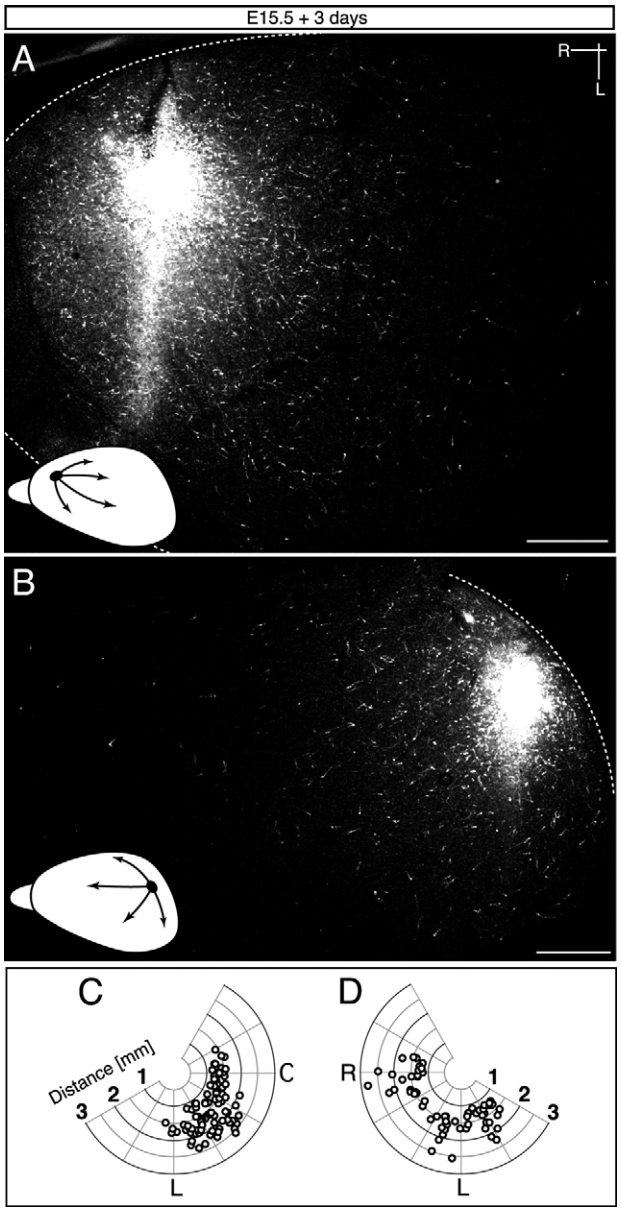

Fig. 7. Dispersion of DiD-labelled GFP neurons in the MZ after the DiD injection into the frontal or occipital cortex, three days after injection (E18.5). (**A**,**B**) Dorsal view of the area around the injection site. Injection was made into the frontal (A) or occipital (B) cortex. Inset diagram illustrates the position of the injection site. (**C**,**D**) Distribution of DiD-labelled GFP neurons after injection into the frontal (C) or occipital (D) cortex. Circles show the positions of DiD-labelled GFP neurons ~1 mm from injection site. Each graph represents pooled data from two independent experiments. The lack of data in regions rostromedial (A,C) or caudomedial (B,D) to the injection site is due to folding of the cortex. R, rostral; C, caudal; L, lateral. Dotted lines show the flat-mount outline. Scale bars: 500 μm.

Rostrocaudally directed tangential migration of cortical interneurons

MDT migration in the MZ has been observed in real-time imaging for both CellTracker-labelled cells (Ang, Jr et al., 2003) and GAD67-GFP cells (Tanaka et al., 2003). Quantitative analysis, however, has not been performed in terms of the directionality of their migration in real time. We show here that MZ GFP neurons primarily migrate rostrocaudally rather than medially, by analysing migrating neurons in cortical flatmounts (Fig. 3). Our results may seem to be inconsistent with the classical view that MZ interneurons migrate dorsomedially (de Carlos et al., 1996; Jimenez

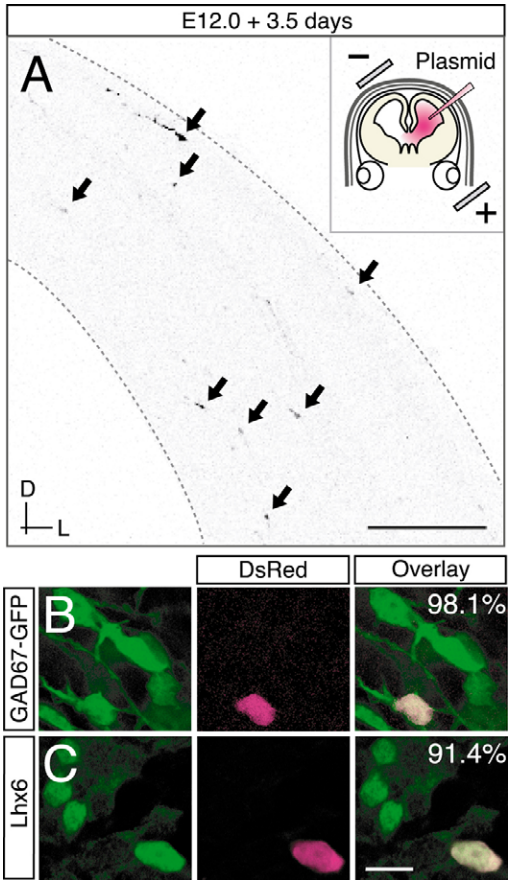

Fig. 8. Distribution and characterization of DsRed-labelled cells 3.5 days after electroporation (E15.5). (**A**) Distribution of DsRed-labelled cells (arrows) in the dorsal cortex in a coronal section. Schematic illustrates GE-directed electroporation at E12.0 (inset). (**B**,**C**) Immunohistochemical characterization of DsRed cells (magenta) in the neocortex. Most DsRed cells in the dorsal cortex were positive for both GAD67-GFP (green in B; 98.1±1%; *n*=207/210 DsRed cells, three brains) and LHX6 (green in C; 91.4±7%; *n*=154/163 DsRed cells, five brains). Dotted lines indicate the section outline. D, dorsal; L, lateral. Scale bars: A, 200 μm; B,C, 10 μm.

et al., 2002; Lavdas et al., 1999; Polleux et al., 2002). This is not the case, however, because, in these previous studies, dorsomedial migration of interneurons was observed in coronal slices, in which rostrocaudal migration of cortical interneurons should not be detected.

MDT migration of MGE-derived interneurons

The mechanisms underlying long-distance MDT migration of interneurons are not known. Accumulating evidence indicates there are temporally and spatially distinct origins for cortical interneurons (Anderson et al., 2001; Anderson et al., 1997; Butt et al., 2005; Lavdas et al., 1999; Nery et al., 2002; Wichterle et al., 2001; Xu et al., 2004), raising the possibility that migration directions might differ for interneurons with different origins. This does not, however, explain the behaviour of DsRed-labelled cells migrating in many directions in the MZ (Fig. 9), because these cells originated from progenitors at a specific site in the basal forebrain, the MGE, and were labelled by electroporation carried out at a specific developmental stage, E12.0. Therefore, although we cannot exclude the possibility that the *DsRed* vector was transferred to several distinct progenitor domains within the MGE, these results suggest that the migration direction of MZ interneurons is independent of their origin.

There are numerous cortical interneuron subtypes with different calcium binding-protein expression, neuropeptide expression, morphology and physiological properties (Kawaguchi and Kubota, 1997; Markram et al., 2004). It is possible that interneurons of each subtype have different migratory pathways, and that the direction of each pathway, which is therefore different for different interneuron subtypes, is strictly regulated by mechanisms present within the cortex. An alternative possibility is that individual neurons can migrate in any direction irrespective of their subtype. Subtype identification of interneurons whose migratory behaviour has been analysed would be necessary to distinguish between these possibilities.

Ventricle-directed migration after dispersion in the MZ

A subset of E18.5 DiD-labelled GFP neurons were observed in the MZ and upper CP, far from injection sites, with ventricle-oriented leading processes (see Fig. S1 in the supplementary material). These may be interneurons that have descended into the CP after completing a tangential dispersion in the MZ. This hypothesis is consistent with previous results. Real-time imaging experiments show that a subset of embryonic interneurons in the MZ migrate into the CP (Ang, Jr et al., 2003; Tanaka et al., 2003). Co-culture experiments (see Fig. S2 in the supplementary material) and a BrdU-labelling study (Hevner et al., 2004) showed postnatal shifts of interneurons from the MZ to the CP.

Waiting period?

DiD-labelling experiments suggest that GABAergic interneurons linger in the MZ for a few days before approaching their final destination, the CP (Figs 6, 7). Several types of developing axons are known to stop growing and wait for the maturation of their targets (Ghosh and Shatz, 1992; O'Leary and Terashima, 1988; Wang and Scott, 2000). By analogy, GABAergic MZ interneurons may require further maturation before continuing their migration, or they may be waiting for the maturation of nearby structures. The validity of this hypothesis awaits further studies.

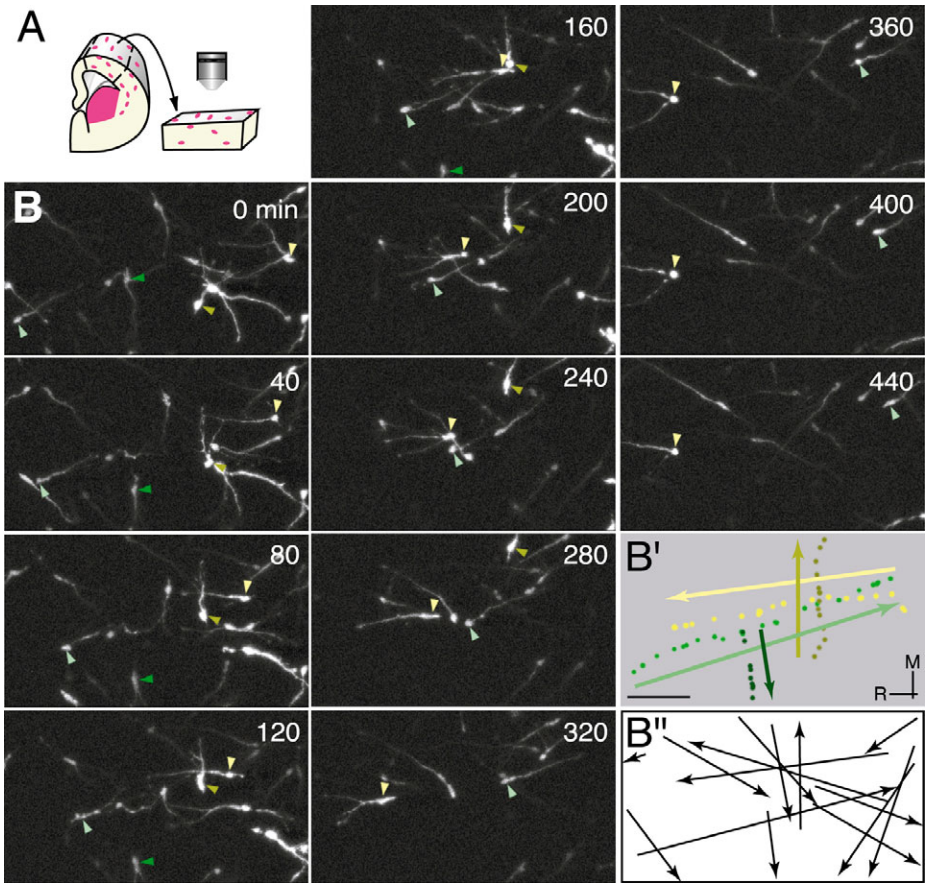

Fig. 9. Time-lapse analysis of MDT migration of DsRed cells in the MZ. (**A**) Schematic of time-lapse imaging in a flat-mount preparation from DsRed-labelled brain. (**B**) Confocal images of DsRed cells in the MZ. The number in the top right corner is the time in minutes. Neurons indicated by arrowheads of the same colour represent the same neurons. (B′) Tracks of the four neurons shown in B. Each dot corresponds to the neurons shown by arrowheads in B and illustrates their positions plotted at 20 minutes intervals. Arrows indicate the direction of migration. (B″) Migration direction of all of the DsRed neurons shown in B. R, rostral; M, medial. Scale bar: 20 μm.

Conclusions

Most cortical interneurons originate in the ventral forebrain and migrate dorsally toward the cortex. The present study shows that some of these migrate tangentially in all directions and in multiple zones, after entering the dorsal cortex. The neurons do not merely wander around locally but migrate over long distances before settling in the CP. This migratory behaviour may contribute to the dispersing and intermixing of cortical interneuron subtypes; it may therefore be important for achieving the final, even distribution of cortical interneuron subtypes throughout the cortex.

We thank Y. Nakaya for help in performing real-time imaging; M. Iwashita for instructions of mouse surgery; Y. Hatanaka for advice in GE-directed electroporation and for critically reading the manuscript; D. Kawauchi for advice in exo utero surgery; V. Pachnis for the rabbit polyclonal anti-LHX6 antibody; J. Miyazaki for the CAG promoter; and N. Yamamoto for critically reading the manuscript. We also thank Y. Zhu, M. Yozu, S. Tada and K. Yamauchi for discussion. This work was supported by SORST from Japan Science Technology Corporation and Grant-in-Aid from the JSPS and MEXT, Japan (1700005 and 17023028). D.H.T. is a pre-doctoral fellow of the JSPS.

Supplementary material

Supplementary material for this article is available at
http://dev.biologists.org/cgi/content/full/133/11/2167/DC1

References

Anderson, S. A., Qiu, M., Bulfone, A., Eisenstat, D. D., Meneses, J., Pedersen, R. and Rubenstein, J. L. (1997). Mutations of the homeobox genes Dlx-1 and Dlx-2 disrupt the striatal subventricular zone and differentiation of late born striatal neurons. *Neuron* **19**, 27-37.

Anderson, S. A., Marín, O., Horn, C., Jennings, K. and Rubenstein, J. L. (2001). Distinct cortical migrations from the medial and lateral ganglionic eminences. *Development* **128**, 353-363.

Ang, E. S., Jr, Haydar, T. F., Gluncic, V. and Rakic, P. (2003). Four-dimensional migratory coordinates of GABAergic interneurons in the developing mouse cortex. *J. Neurosci.* **23**, 5805-5815.

Bielle, F., Griveau, A., Narboux-Neme, N., Vigneau, S., Sigrist, M., Arber, S., Wassef, M. and Pierani, A. (2005). Multiple origins of Cajal-Retzius cells at the borders of the developing pallium. *Nat. Neurosci.* **8**, 1002-1012.

Butt, S. J., Fuccillo, M., Nery, S., Noctor, S., Kriegstein, A., Corbin, J. G. and Fishell, G. (2005). The temporal and spatial origins of cortical interneurons predict their physiological subtype. *Neuron* **48**, 591-604.

de Carlos, J. A., Lopez-Mascaraque, L. and Valverde, F. (1996). Dynamics of cell migration from the lateral ganglionic eminence in the rat. *J. Neurosci.* **16**, 6146-6156.

Fishell, G., Mason, C. A. and Hatten, M. E. (1993). Dispersion of neural progenitors within the germinal zones of the forebrain. *Nature* **362**, 636-638.

Ghosh, A. and Shatz, C. J. (1992). Pathfinding and target selection by developing geniculocortical axons. *J. Neurosci.* **12**, 39-55.

Hatanaka, Y. and Murakami, F. (2002). In vitro analysis of the origin, migratory behavior, and maturation of cortical pyramidal cells. *J. Comp. Neurol.* **454**, 1-14.

Hatanaka, Y., Hisanaga, S., Heizmann, C. W. and Murakami, F. (2004). Distinct migratory behavior of early- and late-born neurons derived from the cortical ventricular zone. *J. Comp. Neurol.* **479**, 1-14.

Hevner, R. F., Daza, R. A., Englund, C., Kohtz, J. and Fink, A. (2004). Postnatal shifts of interneuron position in the neocortex of normal and reeler mice: evidence for inward radial migration. *Neuroscience* **124**, 605-618.

Jimenez, D., Lopez-Mascaraque, L. M., Valverde, F. and De Carlos, J. A. (2002). Tangential migration in neocortical development. *Dev. Biol.* **244**, 155-169.

Kawaguchi, Y. and Kubota, Y. (1997). GABAergic cell subtypes and their synaptic connections in rat frontal cortex. *Cereb. Cortex* **7**, 476-486.

Kriegstein, A. R. and Noctor, S. C. (2004). Patterns of neuronal migration in the embryonic cortex. *Trends Neurosci.* **27**, 392-399.

Lavdas, A. A., Grigoriou, M., Pachnis, V. and Parnavelas, J. G. (1999). The medial ganglionic eminence gives rise to a population of early neurons in the developing cerebral cortex. *J. Neurosci.* **19**, 7881-7888.

Lopez-Bendito, G., Sturgess, K., Erdelyi, F., Szabo, G., Molnar, Z. and Paulsen, O. (2004). Preferential origin and layer destination of GAD65-GFP cortical interneurons. *Cereb. Cortex* **14**, 1122-1133.

Marín, O. and Rubenstein, J. L. (2001). A long, remarkable journey: tangential migration in the telencephalon. *Nat. Rev. Neurosci.* **2**, 780-790.

Marín, O. and Rubenstein, J. L. (2003). Cell migration in the forebrain. *Annu. Rev. Neurosci.* **26**, 441-483.

Markram, H., Toledo-Rodriguez, M., Wang, Y., Gupta, A., Silberberg, G. and Wu, C. (2004). Interneurons of the neocortical inhibitory system. *Nat. Rev. Neurosci.* **5**, 793-807.

Nadarajah, B. and Parnavelas, J. G. (2002). Modes of neuronal migration in the developing cerebral cortex. *Nat. Rev. Neurosci.* **3**, 423-432.

Nadarajah, B., Brunstrom, J. E., Grutzendler, J., Wong, R. O. and Pearlman, A. L. (2001). Two modes of radial migration in early development of the cerebral cortex. *Nat. Neurosci.* **4**, 143-150.

Nadarajah, B., Alifragis, P., Wong, R. O. and Parnavelas, J. G. (2002). Ventricle-directed migration in the developing cerebral cortex. *Nat. Neurosci.* **5**, 218-224.

Nadarajah, B., Alifragis, P., Wong, R. O. and Parnavelas, J. G. (2003). Neuronal migration in the developing cerebral cortex: observations based on real-time imaging. *Cereb. Cortex* **13**, 607-611.

Nery, S., Fishell, G. and Corbin, J. G. (2002). The caudal ganglionic eminence is a source of distinct cortical and subcortical cell populations. *Nat. Neurosci.* **5**, 1279-1287.

Niwa, H., Yamamura, K. and Miyazaki, J. (1991). Efficient selection for high-expression transfectants with a novel eukaryotic vector. *Gene* **108**, 193-199.

Noctor, S. C., Martinez-Cerdeno, V., Ivic, L. and Kriegstein, A. R. (2004). Cortical neurons arise in symmetric and asymmetric division zones and migrate through specific phases. *Nat. Neurosci.* **7**, 136-144.

O'Leary, D. D. and Terashima, T. (1988). Cortical axons branch to multiple subcortical targets by interstitial axon budding: implications for target recognition and "waiting periods". *Neuron* **1**, 901-910.

O'Rourke, N. A., Chenn, A. and McConnell, S. K. (1997). Postmitotic neurons migrate tangentially in the cortical ventricular zone. *Development* **124**, 997-1005.

Parnavelas, J. G. (2000). The origin and migration of cortical neurones: new vistas. *Trends Neurosci.* **23**, 126-131.

Polleux, F., Whitford, K. L., Dijkhuizen, P. A., Vitalis, T. and Ghosh, A. (2002). Control of cortical interneuron migration by neurotrophins and PI3-kinase signaling. *Development* **129**, 3147-3160.

Sussel, L., Marin, O., Kimura, S. and Rubenstein, J. L. (1999). Loss of Nkx2.1 homeobox gene function results in a ventral to dorsal molecular respecification within the basal telencephalon: evidence for a transformation of the pallidum into the striatum. *Development* **126**, 3359-3370.

Tabata, H. and Nakajima, K. (2003). Multipolar migration: the third mode of radial neuronal migration in the developing cerebral cortex. *J. Neurosci.* **23**, 9996-10001.

Takiguchi-Hayashi, K., Sekiguchi, M., Ashigaki, S., Takamatsu, M., Hasegawa, H., Suzuki-Migishima, R., Yokoyama, M., Nakanishi, S. and Tanabe, Y. (2004). Generation of reelin-positive marginal zone cells from the caudomedial wall of telencephalic vesicles. *J. Neurosci.* **24**, 2286-2295.

Tamamaki, N., Yanagawa, Y., Tomioka, R., Miyazaki, J., Obata, K. and Kaneko, T. (2003). Green fluorescent protein expression and colocalization with calretinin, parvalbumin, and somatostatin in the GAD67-GFP knock-in mouse. *J. Comp. Neurol.* **467**, 60-79.

Tanaka, D., Nakaya, Y., Yanagawa, Y., Obata, K. and Murakami, F. (2003). Multimodal tangential migration of neocortical GABAergic neurons independent of GPI-anchored proteins. *Development* **130**, 5803-5813.

Tsunekawa, N., Yanagawa, Y. and Obata, K. (2005). Development of GABAergic neurons from the ventricular zone in the superior colliculus of the mouse. *Neurosci. Res.* **51**, 243-251.

Wang, G. and Scott, S. A. (2000). The "waiting period" of sensory and motor axons in early chick hindlimb: its role in axon pathfinding and neuronal maturation. *J. Neurosci.* **20**, 5358-5366.

Wichterle, H., Turnbull, D. H., Nery, S., Fishell, G. and Alvarez-Buylla, A. (2001). In utero fate mapping reveals distinct migratory pathways and fates of neurons born in the mammalian basal forebrain. *Development* **128**, 3759-3771.

Xu, Q., Cobos, I., De La Cruz, E., Rubenstein, J. L. and Anderson, S. A. (2004). Origins of cortical interneuron subtypes. *J. Neurosci.* **24**, 2612-2622.